Controls on permeability heterogeneity in the Tocito Sandstone (Upper Cretaceous), northwest New Mexico

Mark R. Lambert, Rex D. Cole, and Peter S. Mozley

1997, pp. 217-228. https://doi.org/10.56577/FFC-48.217

in:

Mesozoic Geology and Paleontology of the Four Corners Area, Anderson, O.; Kues, B.; Lucas, S.; [eds.], New Mexico Geological Society 48th Annual Fall Field Conference Guidebook, 288 p. https://doi.org/10.56577/FFC-48

This page is intentionally left blank to maintain order of facing pages.

CONTROLS ON PERMEABILITY HETEROGENEITY IN THE TOCITO SANDSTONE (UPPER CRETACEOUS), NORTHWEST NEW MEXICO

MARK R. LAMBERT[1], REX D. COLE[2] and PETER S. MOZLEY[3]

[1]Mobil Exploration and Producing, U.S., P.O. Box 633, Midland, TX 79702; [2]Department of Physical and Environmental Sciences, Mesa State College, Grand Junction, CO 81502; [3]Department of Earth and Environmental Science, New Mexico Tech, Socorro, NM 87801

Abstract—The Tocito Sandstone Lentil of the Mancos Shale is an Upper Cretaceous (Coniacian) shallow-marine sandstone and mudrock complex that is a major hydrocarbon producer in the San Juan Basin. Most Tocito pay intervals show significant variations in reservoir heterogeneity at a variety of scales. The results of this study strongly suggest that permeability heterogeneity at the macroscopic scale (i.e., well-to-well scale) is largely controlled by lithofacies variations. This conclusion is based on a systematic analysis of permeability variations in the Tocito. Minipermeameter measurements were conducted on outcrops (21 windows, 2 horizontal transects, and 2 vertical transects) and two shallow cores at Hogback oil field (anticline), and four conventional cores from the deep subsurface. A total of 2649 permeability measurements were made; values ranged from 0.0005 to 17.9 darcies. Overall, the permeability values from outcrop and the shallow subsurface cores are dramatically higher than those from the four deep subsurface cores. Average (geometric) permeability values for the outcrop population and the combined shallow-core populations are 2.0 and 0.7 darcies, respectively, whereas the average for the deep-subsurface cores is only 0.001 darcies. In the outcrop and subsurface, the large- and medium-scale cross-stratified sandstone lithofacies have the highest permeability values, followed by the interbedded sandstone and shale, ripple cross-stratified sandstone, and the muddy bioturbated sandstone lithofacies. Siltstone and mudstone interbeds, laminations, and mud drapes are also common in the Tocito. These mudrocks, which have greatly reduced permeabilities, create significant flow barriers and baffles and compartmentalize the Tocito both vertically and laterally. Petrographic examination indicates that permeability enhancement in outcrop and the shallow subsurface is due to dissolution of calcite cement and framework grains by meteoric water, plus microfracturing produced by weathering and decompaction.

INTRODUCTION

The Tocito Sandstone Lentil of the Upper Cretaceous Mancos Shale is a major oil reservoir in the San Juan Basin, New Mexico (Fig. 1). As of early 1992, 117 million barrels of oil (MBO) and 79 billion cubic feet of gas (BCFG) have been produced in the San Juan Basin from the Tocito (Bottjer and Stein, 1994). This accounts for approximately 81% of the oil produced from the San Juan Basin (Rice, 1983). Estimates of undiscovered conventional oil and gas from the Tocito are 9.3 MBO and 46.6 BCFG (Powers, 1993). Efforts at secondary and tertiary recovery from Tocito Sandstone reservoirs have been disappointing due to early water breakthroughs (Fassett et al., 1987), most likely the result of significant reservoir heterogeneity.

Objectives

To enhance understanding of permeability heterogeneity within the Tocito interval, a detailed surface and subsurface investigation was conducted in 1992–93, with subsequent work in 1994 and 1995. The principal objectives were to determine (1) the effect of facies architecture on porosity and permeability heterogeneity; (2) the effect of diagenesis on porosity and permeability heterogeneity; and (3) the extent to which outcrop sections reflect subsurface conditions; i.e., the degree of "data portability" from outcrop to reservoir. The majority of results are given in Lambert (1993), with subsequent documentation in Lambert et al. (1995, 1996). The surface phase of the investigation was conducted at Hogback oil field (Fig. 1), where the Tocito forms a network of three-dimensional outcrops (Riley, 1993). The subsurface investigation included two shallow, "behind-the-outcrop" core holes at Hogback oil field (HOF-2 and HOF-3; see Fig. 1) and four deep subsurface cores (Navajo Tribal F-151, Navajo Tribal E-8, Navajo Tribal H-2, Gallegos Canyon 250) from the Many Rocks, Cha Cha, Totah and Gallegos Canyon fields, respectively (Fig. 1). Additional study of three cores from Angel Peak field (Angel Peak B-37, Martin Gas Unit C-1, and Newsom A-3E) was also performed; however, discussion of these data are beyond the scope of the present paper.

Methods

Outcrop permeability measurements at Hogback oil field were collected at 21 grid-like windows, two vertical transects, and two horizontal transects. Locations for the outcrop study sites were based on the facies-architecture interpretations of Riley (1993). Within the Hogback oil field, the Tocito consists of two major sandstone-dominated intervals of unequal thickness separated by a thin, discontinuous, phosphatic mudrock interval. Windows 1–3 are located in the sandstone above the phosphatic mudstone (i.e., "upper" Tocito), whereas windows 5–9 are in the lower sandstone interval ("lower" Tocito). Window 4 is positioned in the phosphatic mudrock interval. Windows 10–21 were located in outcrops of the "upper" Tocito along the northern banks of the Chaco River. The two vertical outcrop transects, plus a horizontal transect ("lower" Tocito) are near windows 1–9. The second horizontal transect ("upper" Tocito) is located along the Chaco River outcrops near windows 10–21. For the majority of the windows, the spacings between measurements ranged between 0.3 and 1.0 ft horizontally and vertically, irrespective of sedimentary structures. In window 8, however, permeability measurements followed cross-stratal foresets in sandstone. Measurement intervals for the vertical and lateral transects ranged between 0.25 and 2.5 ft.

Three probe permeameters were used for data collection: an Edinburgh Petroleum Services (EPS) mechanical minipermeameter; a Temco digital minipermeameter; and a scanning minipermeameter developed at the New Mexico Petroleum Recovery Research Center. Probe permeameters estimate nondirectional (radial flow) permeability by injection of dry gas at a constant pressure into a rock using a hollow probe tip that is pressed against the rock face. Prior to analysis, individual measurement sites were cleaned (wire brush and/or chisel) to remove weathered materials or stains. Gas flow rate through the probe tip into the rock was measured by either a mechanical rotameter (EPS instrument) or digital flow meter (Temco instrument). By knowing the injection pressure through the probe tip, the gas flow rate, temperature conditions and atmospheric pressure, permeability was calculated using empirical equations presented by Goggin et al. (1988b); see Lambert (1993) for additional details.

For the EPS and Temco instruments, the lower limit of investigation is approximately 0.005 darcies, whereas the upper limits of measurement are about 5.1 and 18 darcies, respectively. Prior to field work, both the EPS and Temco permeameters were calibrated using core plugs from homogeneous sandstone with known permeabilities. The computer-controlled scanning minipermeameter, which was described in detail by Heller (1992), Ali (1993), and Lambert (1993), was used for most of the detailed core analysis. For this instrument, the lower limit of detection is 0.0001 darcies, whereas the upper limit is approximately 8.0 darcies. As shown in Table 1, the upper detection limit (5.145 darcies) was commonly exceeded during some of the outcrop measurements with the EPS permeameter. Correspondingly, statistical analysis of data sets containing these "truncated maximum values" (windows 1, 5, 7, 9, 12 and 21) will be distorted.

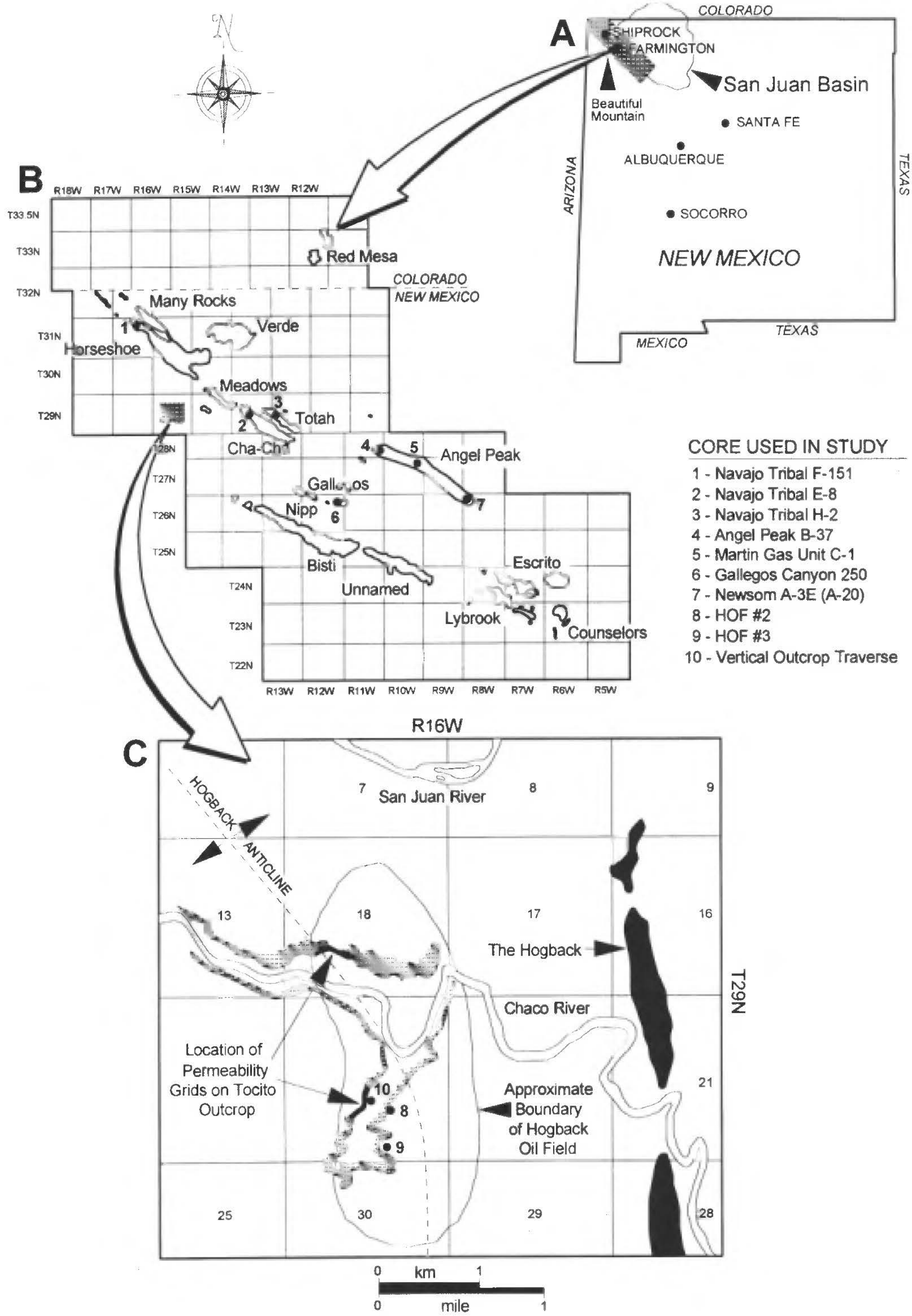

FIGURE 1. Index maps illustrating locations of outcrops and cores used in this study.

GEOLOGIC SETTING

The Tocito Sandstone Lentil of the Mancos Shale is an Upper Cretaceous (Coniacian) shallow-marine sandstone and mudrock complex deposited along the western margin of the Western Interior seaway in northwestern New Mexico and southwestern Colorado (Fig. 1). Depending on location within the San Juan Basin and Four Corners platform, the Tocito overlies either the Gallup Sandstone, Crevasse Canyon Formation, the Pescado Tongue of the Mancos Shale, or the Juana Lopez Member of Mancos Shale (Fig. 2), and is overlain by the Mulatto Tongue of the Mancos Shale. Stratigraphic and sedimentologic interpretations of the Tocito interval have been discussed by numerous workers (see Molenaar, 1983a, 1983b; Tillman, 1985a, 1985b; Jennette et al., 1991; Nummedal and Riley, 1991; Riley, 1993; Bottjer and Stein, 1994; Valasek, 1995; Jennette and Jones, 1995; Nummedal and Molenaar, 1995; and Molenaar et al., 1996, for recent reviews). In summary, results of this work show that the Tocito includes more than a dozen transgressive sand bodies (12 to 31 mi long, 3 to 6 mi wide, and 33 to 66 ft thick) that stack stratigraphically to the southwest. Deposition of the Tocito occurred in shallow-marine, shoreface and estuarine settings, with sediment transport by tidal and storm-generated episodic currents. There is a major unconformity at the base of the Tocito, which has been interpreted as either a sequence boundary created by incised valley-formation or as a sequence boundary produced by marine erosion acting on a tectonically active sea-

TABLE 1. Statistical summary of permeability data generated during study.

Data Set	N	Min.	Med.	Max.	Arith. Mean	Geo. Mean	Std. Dev.	Skew.	Kurt.	Inst.
General Populations										
Total Population	2649	<0.001	2.472	17.876	2.528	0.628	2.147	0.809	4.634	E, T, S
All Outcrop Data	842	0.004	3.247	17.876	3.114	2.032	1.891	1.626	12.677	E, T
Shallow Subsurface Cores	1629	<0.001	2.197	9.114	2.488	0.694	2.184	-1.467	4.140	E, S
Deep Subsurface Cores	178	<0.001	<0.001	0.561	0.025	0.001	0.068	4.420	27.136	E
Window Data										
Total Window Data (1-21)	705	0.004	3.216	>5.145	2.998	2.119	1.385	-0.545	2.588	E
No. 1 (ISS Lithofacies)	25	0.005	2.670	>5.145	2.722	0.784	2.028	-0.197	1.447	E
No. 2 (ISS Lithofacies)	15	0.659	3.401	4.497	3.201	2.858	1.260	-0.688	2.267	E
No. 3 (MBS Lithofacies)	30	0.004	0.068	4.374	1.202	0.181	1.494	0.732	1.891	E
No. 4 (PNM Lithofacies)	25	0.013	0.571	2.012	0.568	0.248	0.560	0.733	2.729	E
No. 5 (RCLS Lithofacies)	18	0.038	2.145	>5.145	2.752	1.923	1.811	0.314	1.554	E
No. 6 (RCLS Lithofacies)	14	0.011	0.692	1.158	0.574	0.184	0.513	-0.106	1.174	E
No. 7 (GS Lithofacies)	100	0.010	2.773	>5.145	2.838	1.943	1.703	-0.019	1.642	E
No. 8 (GS Lithofacies)	57	1.389	3.206	4.826	3.162	3.077	0.709	-0.126	2.928	E
No. 9 (GS Lithofacies)	112	0.972	4.036	>5.145	3.900	3.751	0.950	-0.823	3.431	E
No. 10 (LSCSS Lithofacies)	33	1.389	2.979	4.363	3.010	2.924	0.702	-0.114	2.634	E
No. 11 (BMS Lithofacies)	20	2.058	2.513	3.267	2.569	2.550	0.331	0.626	2.959	E
No. 12 (LSCSS Lithofacies)	41	2.521	3.895	>5.145	3.839	3.770	0.723	-0.049	2.319	E
No. 13 (LSCSS Lithofacies)	28	1.204	3.072	4.368	2.960	2.881	0.645	-0.416	3.593	E
No. 14 (ISS Lithofacies)	15	0.033	1.796	3.602	1.747	1.094	1.036	-0.123	2.353	E
No. 15 (LSCSS Lithofacies)	14	3.216	4.222	4.739	4.099	4.067	0.509	-0.631	2.244	E
No. 16 (LSCSS Lithofacies)	9	3.025	3.597	3.982	3.524	3.511	0.323	-0.125	2.013	E
No. 17 (LSCSS Lithofacies)	9	2.089	2.727	2.923	2.615	2.596	0.321	-0.800	2.113	E
No. 18 (LSCSS Lithofacies)	78	1.945	3.491	4.677	3.412	3.333	0.709	-0.207	2.312	E
No. 19 (LSCSS Lithofacies)	18	1.147	2.637	4.106	2.722	2.565	0.908	-0.017	1.895	E
No. 20 (LSCSS Lithofacies)	16	1.261	2.505	4.379	2.517	2.399	0.782	0.429	3.382	E
No. 21 (MSCSS Lithofacies)	28	1.291	3.838	>5.145	3.690	3.590	0.773	-1.002	4.683	E
Vertical and Horizontal Outcrop Transects										
Measured Section No. 1	20	0.049	1.368	6.079	2.181	1.124	2.023	0.738	2.228	E
Measured Section No. 2	25	0.005	1.701	11.142	2.582	0.472	3.171	1.400	4.335	T
Horizontal Transect No. 1	51	0.004	3.429	17.876	4.419	1.562	4.483	1.248	3.939	T
Horizontal Transect No. 2	41	1.757	4.619	8.538	4.722	4.437	1.644	0.544	3.042	T
Vertical Core Transects										
HOF-2 (Slabs)	1555	<0.001	2.218	9.114	2.525	0.690	2.214	0.561	2.347	S
HOF-2 (Plugs)	39	0.003	2.056	3.624	1.812	0.883	1.111	-0.348	1.961	E
HOF-3 (Plugs)	35	0.005	1.744	4.356	1.744	0.710	1.333	0.161	1.883	E
Navajo Tribal F-151	51	0.001	0.014	0.275	0.041	0.014	0.063	2.309	7.783	E
Navajo Tribal E-8	14	<0.001	0.009	0.167	0.033	0.005	0.048	1.749	5.235	E
Navajo Tribal H-2	14	<0.001	0.051	0.561	0.130	0.007	0.170	1.240	3.746	E
Gallegos Canyon 250	99	<0.001	<0.001	0.035	0.002	0.001	0.006	3.784	18.227	E

Abbreviations: N = number of observations in data set; Min. = minimum; Med. = median; Max. = maximum; Arith. = arithmetic; Geo. = geometric; Std. Dev. = standard deviation; Skew. = skewness; Kurt. = kurtosis; Inst. = permeameters used (E = Edinburgh Petroleum Services, T = Temco, and S = scanning). Lithofacies abbreviations are explained in text.

All values except N are in darcies.

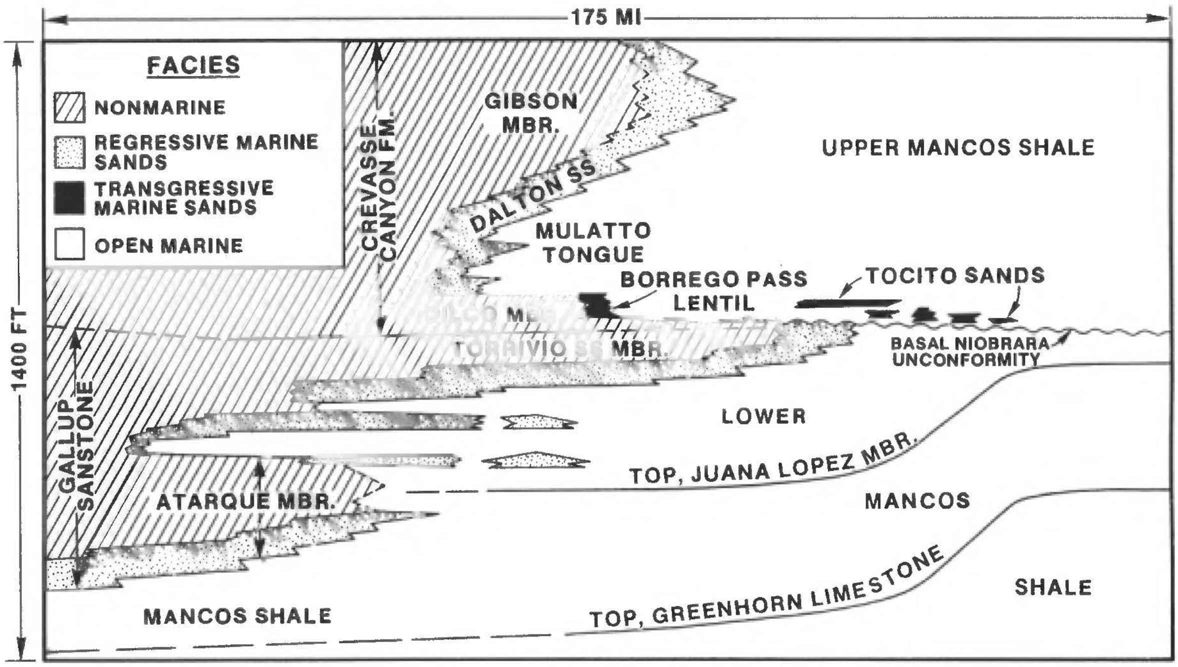

FIGURE 2. North–south stratigraphic cross section of the San Juan Basin showing position of Tocito Sandstone Lentil of the Mancos Shale with respect to other Upper Cretaceous units. Modified from Molenaar (1973).

bottom high. Additional unconformities (sequence boundaries) have been identified within the Tocito itself.

LITHOFACIES

Riley (1993) identified nine major lithofacies in the Tocito Sandstone in outcrop and shallow cores at Hogback oil field: (1) glauconitic sandstone (GS); (2) large-scale cross-stratified sandstone (LSCSS); (3) medium-scale cross-stratified sandstone (MSCSS); (4) interbedded sandstone and shale (ISS); (5) muddy bioturbated sandstone (MBS); (6) ripple cross-laminated sandstone (RCLS); (7) pebbly sandstone (PS); (8) phosphatic nodular mudstone (PNM); and (9) sandy shale (SS). A set thickness of 3.3 ft differentiates medium-scale (less than 3.3 ft) from the large-scale cross-bedded sandstone facies. The GS, LSCSS, MSCSS and PS lithofacies were produced by subaqueous bedform migration (sand-ridge complexes) induced by strong storm and tidal currents operating in an estuarine to inner-shelf setting. The ISS, BMS and RCLS lithofacies were deposited in a similar setting by lower energy currents. Characteristics of the PNM lithofacies suggest lower energy depositional conditions, possibly produced by vertical sediment aggradation in abandoned tidal channels or between estuarine bars, whereas the SS lithofacies was the product of shallow-shelf deposition (Riley, 1993; Nummedal and Molenaar, 1995).

Description

The *GS lithofacies* consists of medium- to coarse-grained, moderately well sorted sandstone composed of quartz, feldspar and glauconite (up to 25%), which forms oversized peloids. It is characterized by medium- to large-scale trough and tabular-tangential cross-stratification and sigmoidal cross-stratification; foresets are usually accentuated by mud drapes. Bioturbation in the GS lithofacies is rare. The *LSCSS lithofacies* consists of medium- to coarse-grained, well-sorted sandstone characterized by large-scale trough and tabular-tangential cross-stratification, soft-sediment deformation structures, and reactivation surfaces with mud drapes. Locally, cross-bed sets in the LSCSS lithofacies form distinct tidal bundles and bundle sequences; bioturbation is rare. The *MSCSS lithofacies* consists of medium- to coarse-grained, well-sorted sandstone containing scattered quartz and chert granules and pebbles, phosphate nodules (burrow casts), glauconite peloids and mud rip-up clasts. Sedimentary structures in the MSCSS lithofacies include sets of trough and tabular cross-stratification. Foresets in the MSCSS lithofacies can be tangential to planar and the toesets (if preserved) are occasionally rippled and interbedded with thin mud drapes. Bioturbation in the MSCSS lithofacies is rare. The *ISS lithofacies* consists of fine- to medium-grained sandstone beds intercalated with siltstone and muddy, fine-grained sandstone. Sandstone beds, which range in thickness from 0.1 to 1 ft, contain low-angle cross-stratification, ripple cross-stratification, and high-angle tabular cross-stratification (rare). Mudrock intervals are usually less than 0.2 ft thick and contain lenticular, wavy, and flaser bedding (rare). The ISS lithofacies has variable amounts of bioturbation, mud rip-up clasts, shell fragments, glauconite, and phosphatic lithoclasts. The *MBS lithofacies* consists of fine- to medium-grained, poorly to moderately sorted, intensely bioturbated sandstone. Framework grains consist of quartz and feldspar with up to 5% glauconite, and dispersed mud. Remnant sedimentary structures include low-angle stratification, tabular-tangential and tabular-planar cross-stratification and trough cross-stratification. The *RCLS lithofacies* consists of fine- to medium-grained, moderately sorted sandstone that exhibits thin sets of combined-flow ripple lamination and wave-ripple lamination. Thin mud drapes accentuate the stratification. Inoceramid shell fragments are locally abundant in the RCLS lithofacies, and bioturbation is variable. The *PS lithofacies* is a minor element within the Tocito. Sandstone in this lithofacies is fine to coarse grained, poorly to moderately sorted, and contains abundant (up to 25%) granules and pebbles of quartz, chert, phosphate and shell fragments. Sedimentary structures include low-angle stratification, planar cross-stratification and trough cross-stratification. Some intervals appear structureless to graded. Burrowing in the PS lithofacies is variable. The *PNM lithofacies* is very heterolithic, composed of muddy, very fine- to coarse-grained, glauconitic sandstone and sandy, glauconitic mudstone that is usually intensely bioturbated. Pebble- to granule-sized phosphate clasts (probably reworked phosphatic burrows), shark teeth and mollusk fragments are common in the PNM lithofacies. The *SS lithofacies* consists of bioturbated, carbonaceous, slightly glauconitic siltstone, mudstone and very fine- to medium-grained sandstone. Stratification is generally indistinct because of bioturbation. Carbonaceous particles are fragments and are up to one centimeter across.

Abundance and architecture

The cross sections of Riley (1993) at Hogback oil field (Fig. 3) and along the Chaco River show that lithofacies abundance depends on the orientation of the observational window (i.e., cross section orientation) with respect to sediment transport direction. In cross-section A–A' (Fig. 3), which is oriented perpendicular to the average sediment transport direction, the relative proportions of the GS, LSCSS, MSCSS, ISS, MBS, RCLS, PS and PNM lithofacies are 5, 10, 30, 35, 15, 3, 0 and 2%, respectively, whereas in cross-section B–B', which is oriented oblique to the current flow, the relative proportions of these lithofacies are 0, 15, 45,

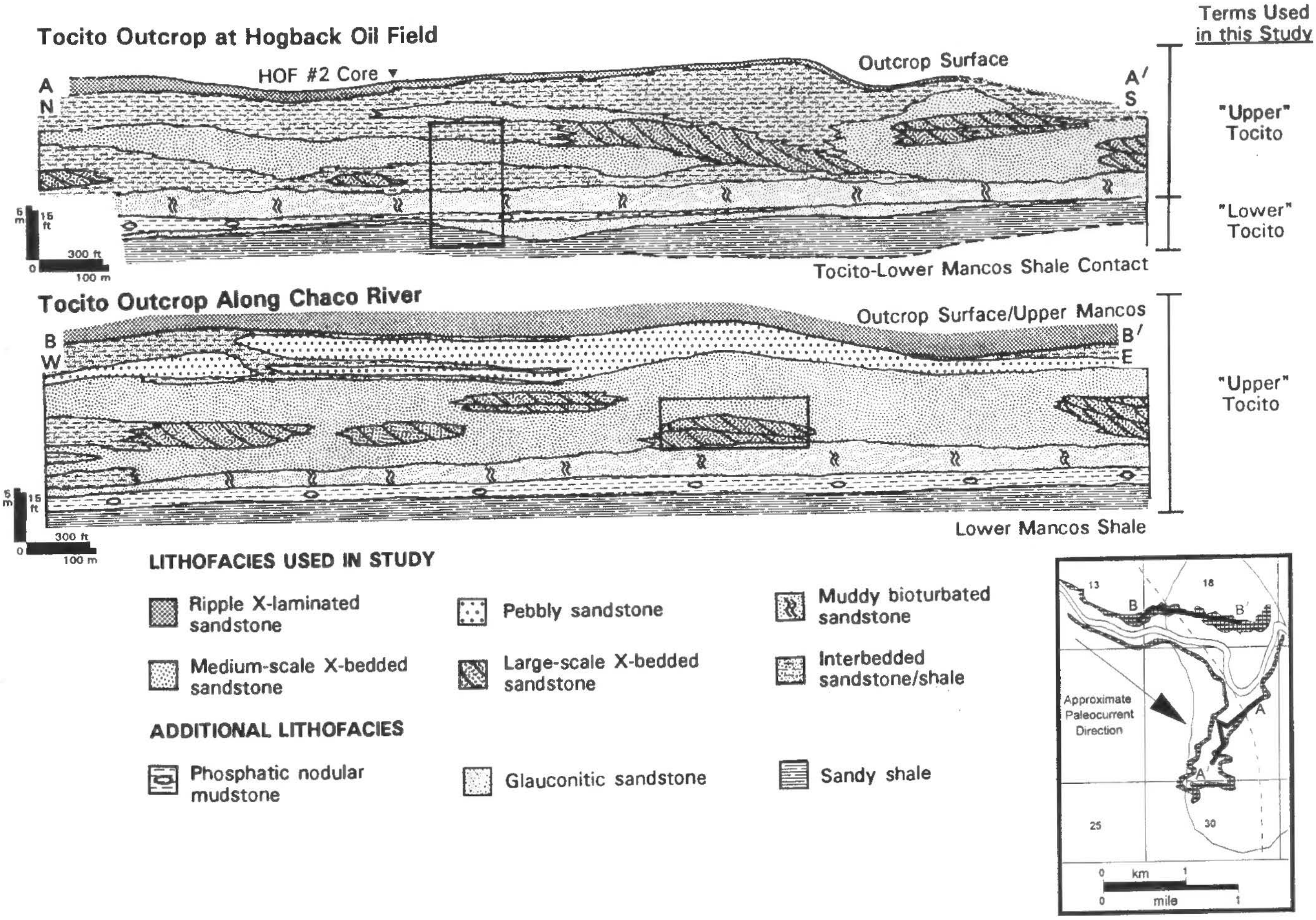

FIGURE 3. North–south and east–west cross sections of Tocito Sandstone at Hogback oil field (modified from Riley, 1993). The boxes in sections A–A' and B–B' mark locations where outcrop permeability measurements (windows, vertical transects and lateral transects) were made.

5, 10, 10, 15 and 0%, respectively. Cross-sections A–A' and B–B' also show that specific Tocito lithofacies have variable lateral continuities. For example, in a down-current direction (B–B'), the LSCSS lithofacies forms thin (2–10 ft) lenses 250 to 600 ft across, encapsulated mainly in the MSCSS lithofacies, whereas in the current-perpendicular view (A–A'), these same lenses are up to 1500 ft across and associated laterally with the MSCSS lithofacies, and also the ISS lithofacies. It is clear from cross-sections A–A' and B–B' that significant lateral lithofacies variations are to be expected at megascopic (field), macroscopic (interwell) and mesoscopic (wellbore) scales.

PETROGRAPHY AND DIAGENESIS

Sandstones in the Tocito are mainly arkoses and sub-arkoses (Fig. 4). The principal framework grains are quartz (average = 38%), potassium feldspar (average = 15%), plagioclase (average = 1%) and rock fragments (average = 2%; mainly chert and mudstone clasts). The most abundant non-framework components include detrital/mechanically infiltrated clay (average = 9%), glauconite (average = 3%), carbonate fluorapatite (average = 2%), pyrite (average = 1%), kaolinite (average = 1%), quartz overgrowths (average = 2%) and calcite (average = 10%).

The Tocito has undergone significant diagenetic change, ranging from alterations that occurred shortly after deposition, to those that occurred during deep burial and following uplift and exposure of the current outcrops. The diagenetic history of the Tocito is summarized in Figure 5; see Lambert (1993) for a detailed discussion of Tocito diagenesis. Many of these alterations have had a significant impact on porosity and permeability. In particular, compaction and precipitation of quartz and calcite cements have decreased porosity and permeability, whereas dissolution of framework grains has increased porosity and permeability.

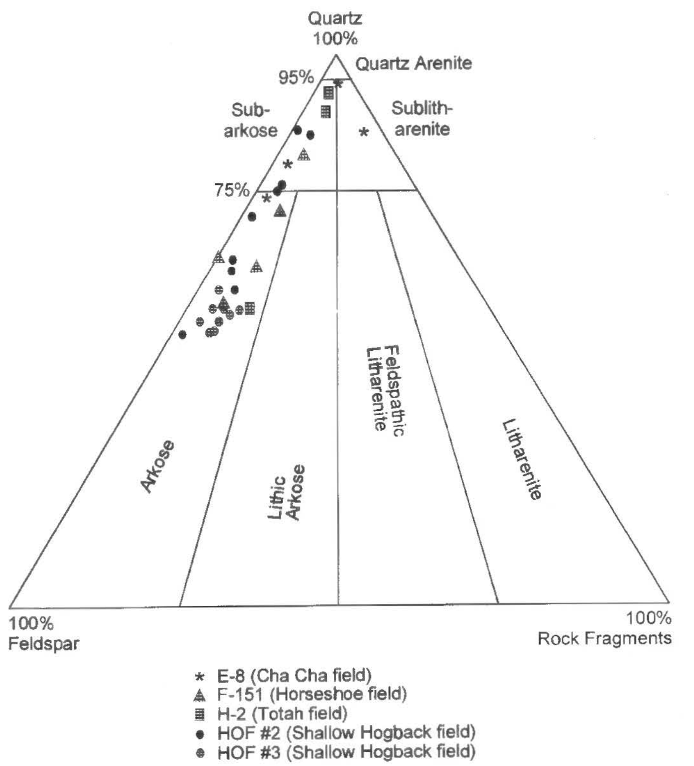

FIGURE 4. Ternary plot showing classification of sandstones for samples from shallow and deep subsurface cores (classification of Folk, 1974).

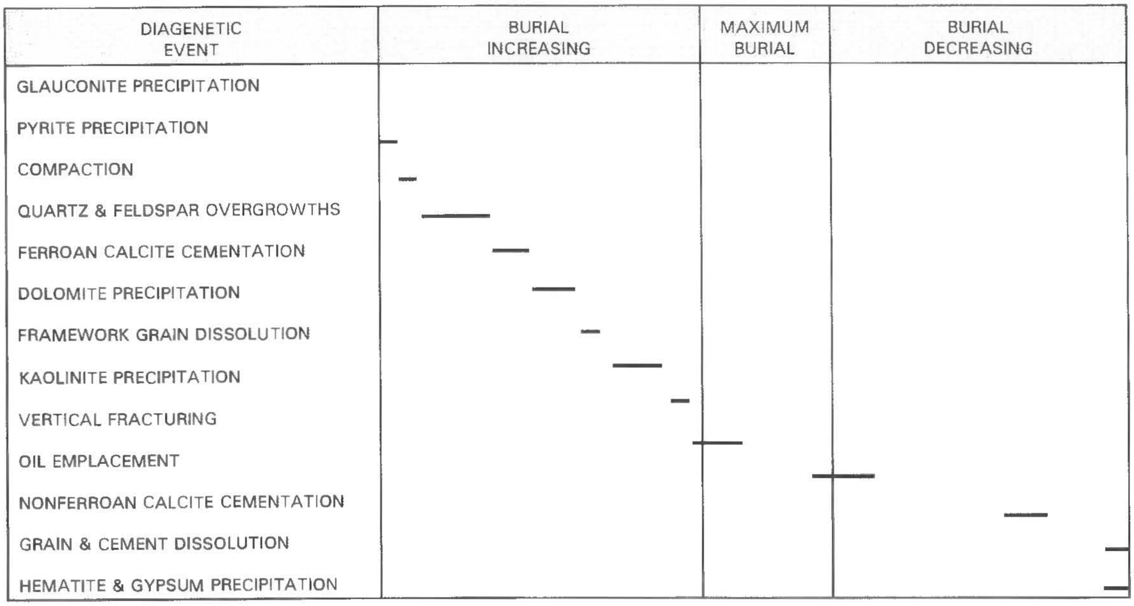

FIGURE 5. Diagenetic history of the Tocito Sandstone. Relatively early alterations are plotted on the left, relatively late toward the right. Some alterations have only affected outcrop and shallow subsurface samples (see text).

Tocito outcrop and shallow subsurface samples have undergone significantly different diagenetic histories than those from the deep subsurface. Late-stage non-ferroan calcite cement is only found in the outcrop and shallow core samples. Likewise, late-stage grain and calcite dissolution only affected outcrop and shallow core samples.

SUMMARY OF PERMEABILITY DATA

The total data set consists of 2649 permeability measurements (Table 1); values range from 0.0005 to 17.9 darcies. Overall, the permeability values from outcrop and the shallow subsurface cores (HOF-2 and HOF-3) are dramatically higher than those from the four deep subsurface cores. Geometric mean values for the combined outcrop and HOF-2-HOF-3 populations are 2.0 and 0.7 darcies, respectively, whereas the mean value for the deep subsurface cores is only 0.001 darcies. The enhanced permeability (and porosity) in the outcrop and shallow cores is most likely due to dissolution of calcite cement and framework grains by meteoric water (see above), plus micro-fracturing produced by decompaction and weathering.

Outcrop

Outcrop data (N = 842) were collected from 21 windows, two measured sections, and two lateral transects. Permeability values range from 0.004 to 17. 9 darcies, with an geometric mean of 2.0 darcies (Table 1). As a whole, values from the windows, measured sections, and lateral transects show similar statistical parameters.

Permeability windows

Permeability windows were generally positioned on a specific lithofacies type or a group of associated lithofacies within the Tocito. It is beyond the scope of this paper to describe the permeability variations observed in the 21 outcrop windows; instead pertinent, representative examples (windows 2, 5, 7, 10, 11, 12, 13 and 14) are summarized below (see Lambert, 1993, for additional details). Permeability measurements for the window sites were made with the EPS instrument.

An example of permeability variations in the ISS lithofacies is documented in window 1 (Fig. 6), which involved 25 permeability measurements in a 2.0 by 2.7 ft area that was positioned nearly perpendicular to the local paleocurrent direction (azimuth = 120–140°). Permeability values in window 1 range from 0.005 to more than 5.1 darcies (upper limit of instrument); the geometric mean is 0.8 darcies. Within this window, clay-poor sandstone intervals are interbedded with clay-rich layers. Permeability values are distinctly lower in the clay-rich intervals (2-4 darcies), compared to the clay-poor intervals (3.9 to more than 5.2 darcies). Permeability contours roughly parallel stratification.

Permeability window 3 (Fig. 7) involved 30 measurements in a 2.7 by 2.5 ft rectangular area of MBS lithofacies; this window was also positioned approximately perpendicular to the local paleocurrent direction. Permeability values range from 0.004 darcies to 4.4 darcies; the geometric mean is 0.2 darcies. Overall, the permeability values increase upward. A mudstone drape splits the window into an upper and lower half. The lower half is characterized by low permeability, but has a localized lens-shaped area with moderate permeability. The upper half of the window has an average permeability that increases from 1.3 darcies just above the mudstone drape to 3.3 darcies near the top of the window. Data from window 3 illustrate how bioturbation can adversely affect permeability in the Tocito, plus how thin mudrock drapes can serve as small-scale permeability baffles or barriers.

Window 5 (Fig. 8), which is orientated parallel to the paleocurrent flow, is a 1.0 by 2.7 ft area of RCLS lithofacies. The 18 measurements taken in window 5 range from 0.04 darcies to more than 5.1 darcies (maximum for instrument used); the geometric mean is 1.9 darcies. Permeability contours in window 5 parallel the stratification. High permeability values along the bottom of the window were taken from highly weathered sandstone; thus, these values are not representative of unweathered ripple cross-laminated sandstones.

Window 7 (Fig. 9) represents a 2.9 by 3.3 ft area of GS lithofacies with large-scale cross stratification oriented parallel to the local paleocurrent direction. Data from window 7 (N = 100 measurements) show a range from 0.01 darcies to more than 5.1 darcies, and an geometric mean of 1.9 darcies. Two relatively impermeable mudstone drapes divide the window into three sandstone sections. The middle sandstone section has a concentric contour pattern with permeability values increasing towards the center. The lower (and thickest) sandstone section is characterized by low permeabilities (1.0 darcies) near the base, high permeabilities (>5 darcies) in the center and moderately high permeabilities (4.0 darcies) at the top. The thinly interbedded sandstone and mudstone interval at the top has an average permeability of 1.2 darcies. The thin sandstone layers have low permeabilities and are resistant to weathering.

Windows 10 through 14 represent five irregularly shaped data-collection areas within a 3.9 by 4.9 ft panel (Fig. 10) located along the north bank of the Chaco River (Fig. 3). Within this panel, which is oriented parallel to the dominant paleocurrent direction, are spectacular exposures of LSCSS lithofacies (windows 10 and 13), LSCSS and MSCSS lithofacies with reactivation surfaces (window 12), MBS lithofacies (window 11) and ISS lithofacies (window 14). Measurements in windows 10, 12 and 13 were made along the large-scale foresets. Values ranged from 1.4 to 4.4 darcies (N = 33; geometric mean = 2.9 darcies) in window 10, from 2.5 to >5.1 darcies (N = 41; geometric mean = 3.8 darcies) in window 12, and from 1.2

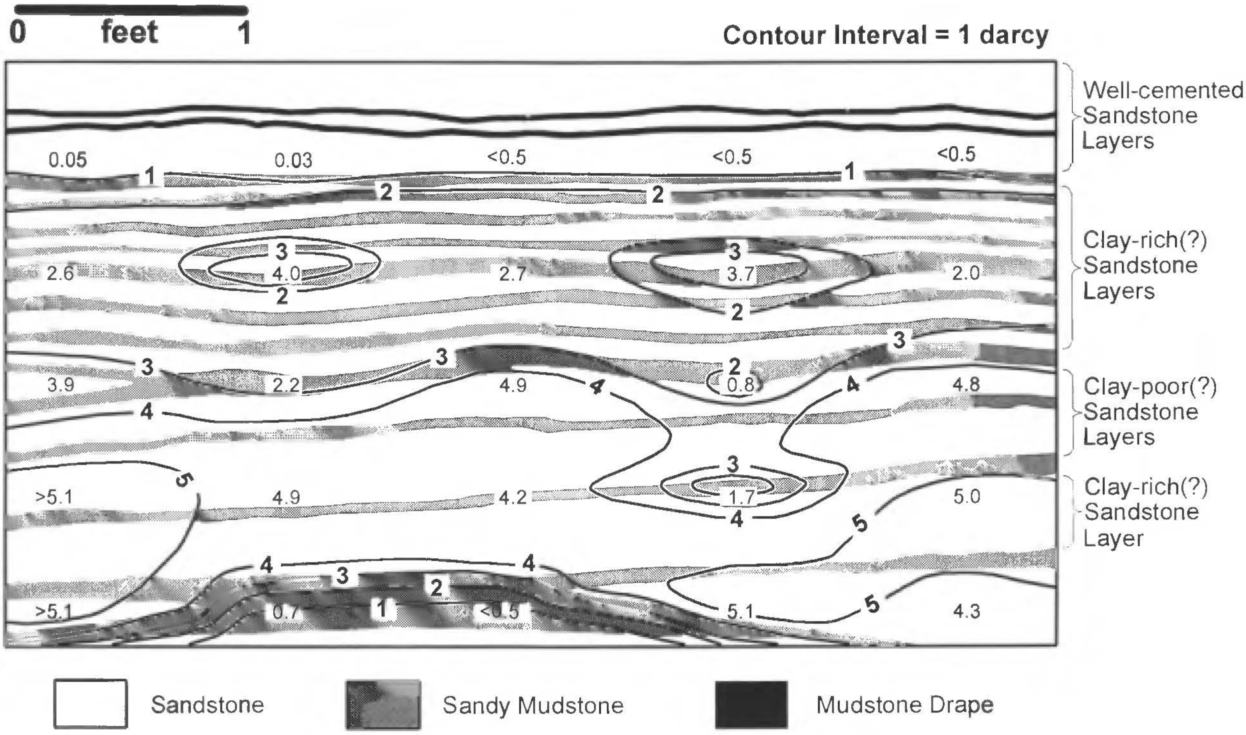

FIGURE 6. Permeability variations within window 1 at Hogback oil field, which consists of interbedded sandstone and mudstone (ISS lithofacies). Window 1 is positioned perpendicular to the local paleocurrent direction. Measurement locations coincide with the decimal points.

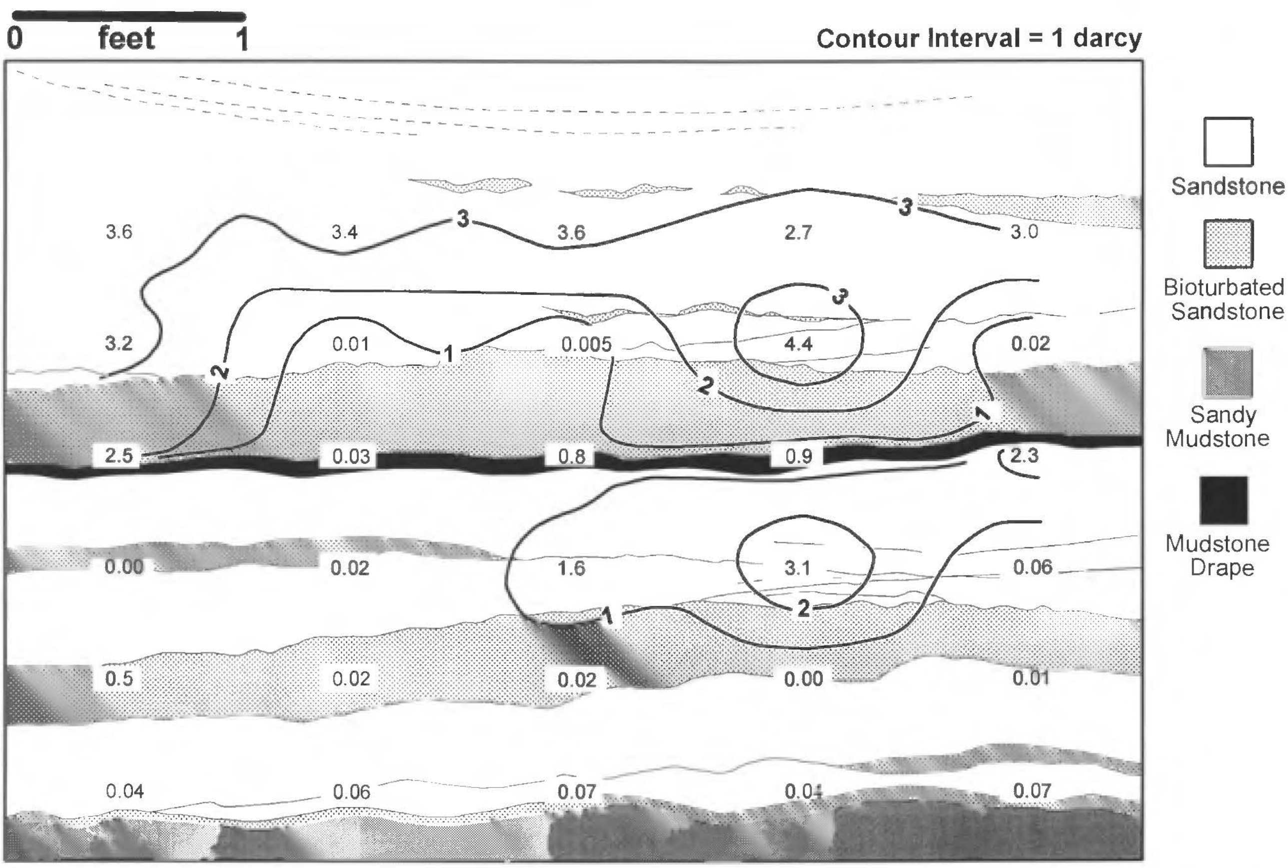

FIGURE 7. Permeability variations within window 3 at Hogback oil field, which consists of muddy bioturbated sandstone (MBS lithofacies). Window 3 is positioned perpendicular to the local paleocurrent direction. Measurement locations coincide with the decimal points.

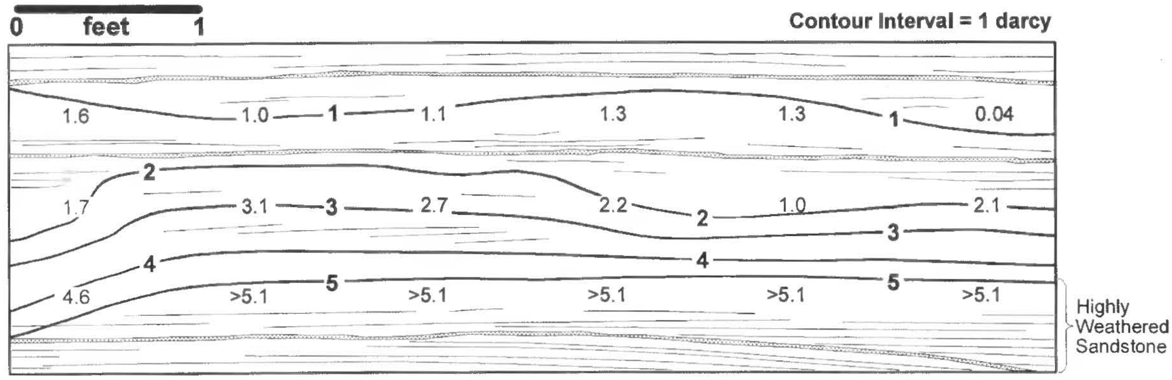

FIGURE 8. Permeability variations within window 5 at Hogback oil field. Rock within window consists of ripple cross-laminated sandstone with thin mudrock interbeds (RCLS lithofacies). Window 5 is positioned perpendicular to the local paleocurrent direction. Measurement locations coincide with the decimal points.

to 4.4 darcies (N = 28; geometric mean = 2.9 darcies) in window 13. Permeability contours are generally oriented parallel to the foreset inclination in windows 10–13. In window 12, a zone of high permeability (4.0–>5.2 darcies) exists in the center of the area, parallel to the reactivation surfaces. Sandstone and mudrock within windows 11 and 14 represent the bioturbated toesets of LSCSS and MSCSS lithofacies (positioned up-current from panel). Permeability values in window 11 are generally homogeneous (range = 2.1–3.3 darcies; geometric mean = 2.6 darcies; N = 20), with relatively higher values near the top of the window. Data from window 14, on the other hand, show extreme heterogeneity; values (N =

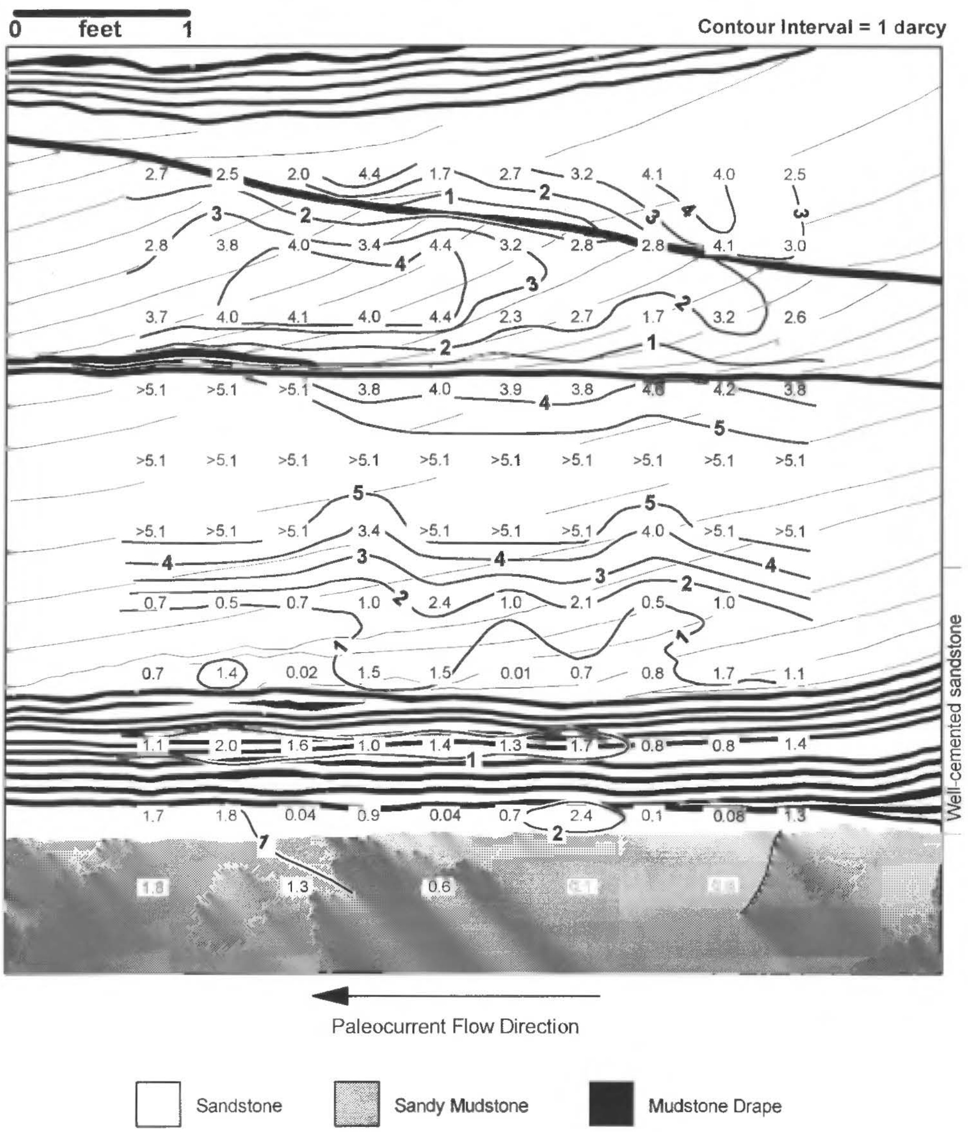

FIGURE 9. Permeability variations within window 7 at Hogback oil field. Rock within window consists of larger-scale cross-stratified sandstone with local shale drapes (MSCSS and LSCSS lithofacies). Window 5 is positioned parallel to the local paleocurrent direction (note orientation of foresets). Measurement locations coincide with the decimal points.

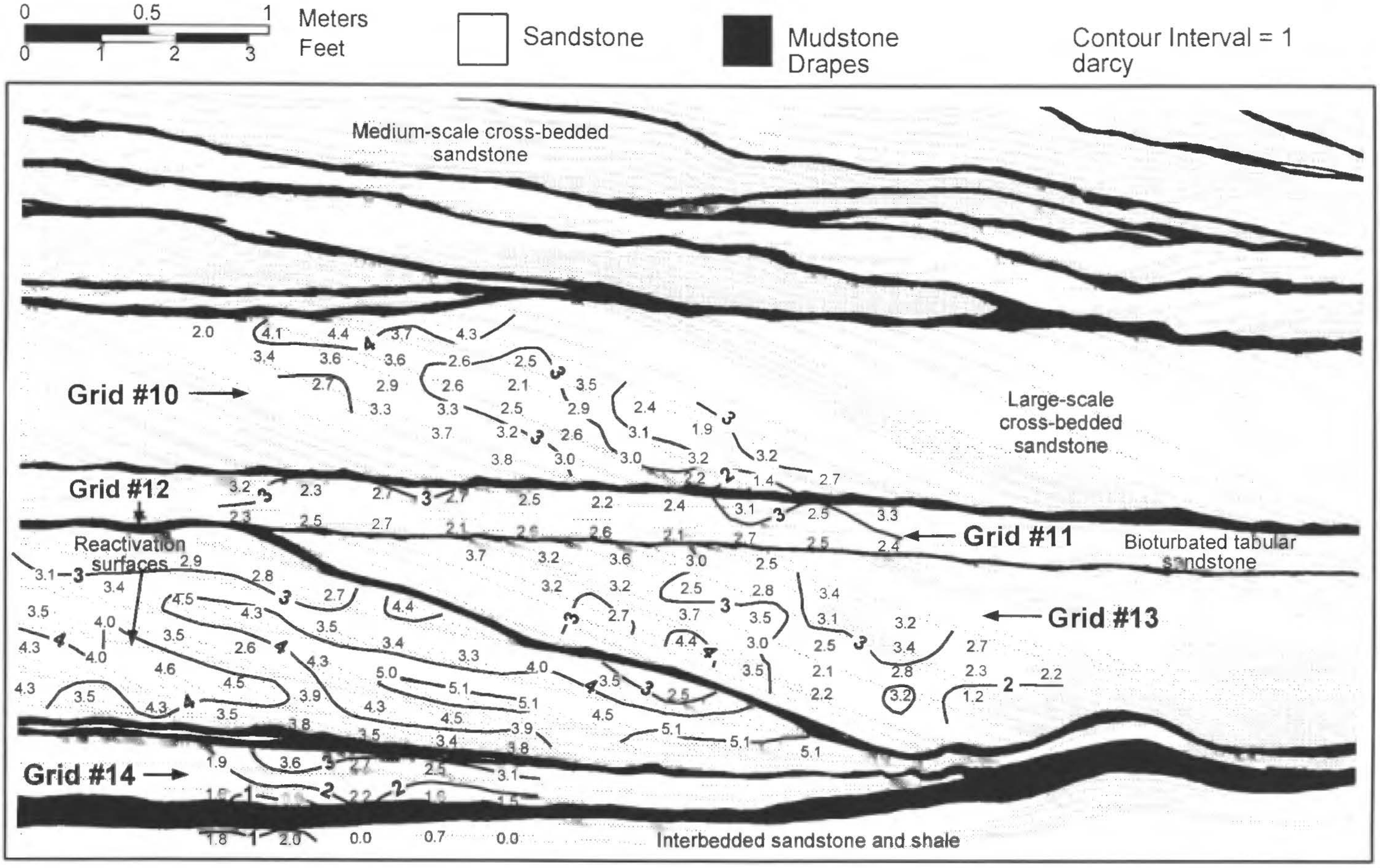

FIGURE 10. Permeability variations in Tocito Sandstone along the Chaco River. This panel contains windows 10-14. Sandstone within panel has large- to medium-scale sets of tabular-tangential and sigmoidal cross-stratification, with common mud drapes and reactivation surfaces. Panel is positioned parallel to the local paleocurrent direction (note orientation of foresets). Measurement locations coincide with the decimal points.

15) range from 0.03 to 3.6 darcies, with an geometric mean of 1.1 darcies. Contour lines through window 14 show a horizontal structure with values increasing upward.

Lateral transects

Two lateral (horizontal) permeability transects were completed during the study. The first transect (125 ft) was in GS lithofacies at the base of the Tocito Sandstone near the window sites at Hogback oil field (see A–A' in Fig. 3), whereas the other transect (41 ft) was in LSCSS and MSCSS lithofacies along the Chaco River (near windows 10–14). The horizontal transect (measurement interval = 2.5 ft) through the GS lithofacies yielded permeability values ranging from 0.004 to 17.9 darcies, with an geometric mean of 1.6 darcies (Table 1). The Chaco River transect (measurement interval = 1.0 ft) yielded values ranging from 1.8 to 8.5 darcies, with an geometric mean value of 4.4 darcies.

Shallow subsurface core

Vertical permeability variations in the Tocito Sandstone at Hogback oil field were defined in two partial measured sections and in shallow core holes HOF-2 and HOF-3; statistical summaries are given in Table 1. The most complete record of vertical permeability variations was generated from the HOF-2 core; thus, in this summary, only these data are discussed. The HOF-2 core is located near the center of Hogback oil field (Fig. 1) approximately 200 ft from the nearest outcrop. Coring started at the surface and continued to approximately 69 ft; see Riley (1993) for details. Permeability measurements were made on clean slabs of the core from 5.0 to 52.7 ft. At each increment station, seven permeability measurements were taken in a 1.5 inch-wide band across the center of the core. These values were averaged arithmetically for plotting (Fig. 11). At each vertical sampling station, lithofacies type, grain size (in phi units), mud content (percent), bioturbation (percent) and cement (percent) were estimated visually (Fig. 11). Gaps in the data are due to missing core or because the core was of poor quality (rubble zones and/or fractured intervals).

The HOF-2 core (Fig. 11) contains most of the lithofacies observed in outcrop (Fig. 3). Permeability values in the HOF-2 core are greatest in the LSCSS (up to 9.0 darcies) and MSCSS lithofacies (3.0 to 6.0 darcies). Mudrock interbeds between sets of LSCSS and MSCSS sandstone are noticeably less permeable; values are usually less than 1.0 darcy. Permeability values in the GS lithofacies range between 0.02 and 1.8 darcies. In the ISS lithofacies, sandstone beds have permeabilities ranging between 2.0 and 5.0 darcies, whereas the intercalated mudrocks are usually less than 1.0 darcy. Permeability values in the RCLS lithofacies are fairly homogeneous, ranging between 0.01 to 0.10 darcies. Permeability values in the MBS lithofacies are erratic (0.001 to 0.1 darcies) and correlate directly with bioturbation intensity. Low permeability intervals are carbonate cemented. The irregular nature of the permeability values in the HOF-2 core shows that a significant amount of heterogeneity exists, especially in lithofacies that are thinly stratified, shale-prone, and/or bioturbated.

Deep subsurface core

Permeability variations in seven cores from producing fields (Fig. 1) were evaluated: Navajo Tribal F-151, Navajo Tribal E-8, Navajo Tribal H-2, Angel Peak B-37, Martin Gas Unit C-1, Gallegos Canyon 250 and Newsom A-3E (A-20). The bulk of the work was performed on the Solar Petroleum Navajo Tribal F-151 core, as discussed below. Information on the remaining cores can be found in Lambert (1993).

The Tocito in the F-151 core consists of thinly interstratified fine- to coarse-grained, burrowed to cross-stratified sandstone and muddy sandstone, and sandy siltstone (Fig. 12), ranging in depth from 921 to 946 ft; ISS, MSCSS, RCLS, and MBS lithofacies dominate. Additional information on

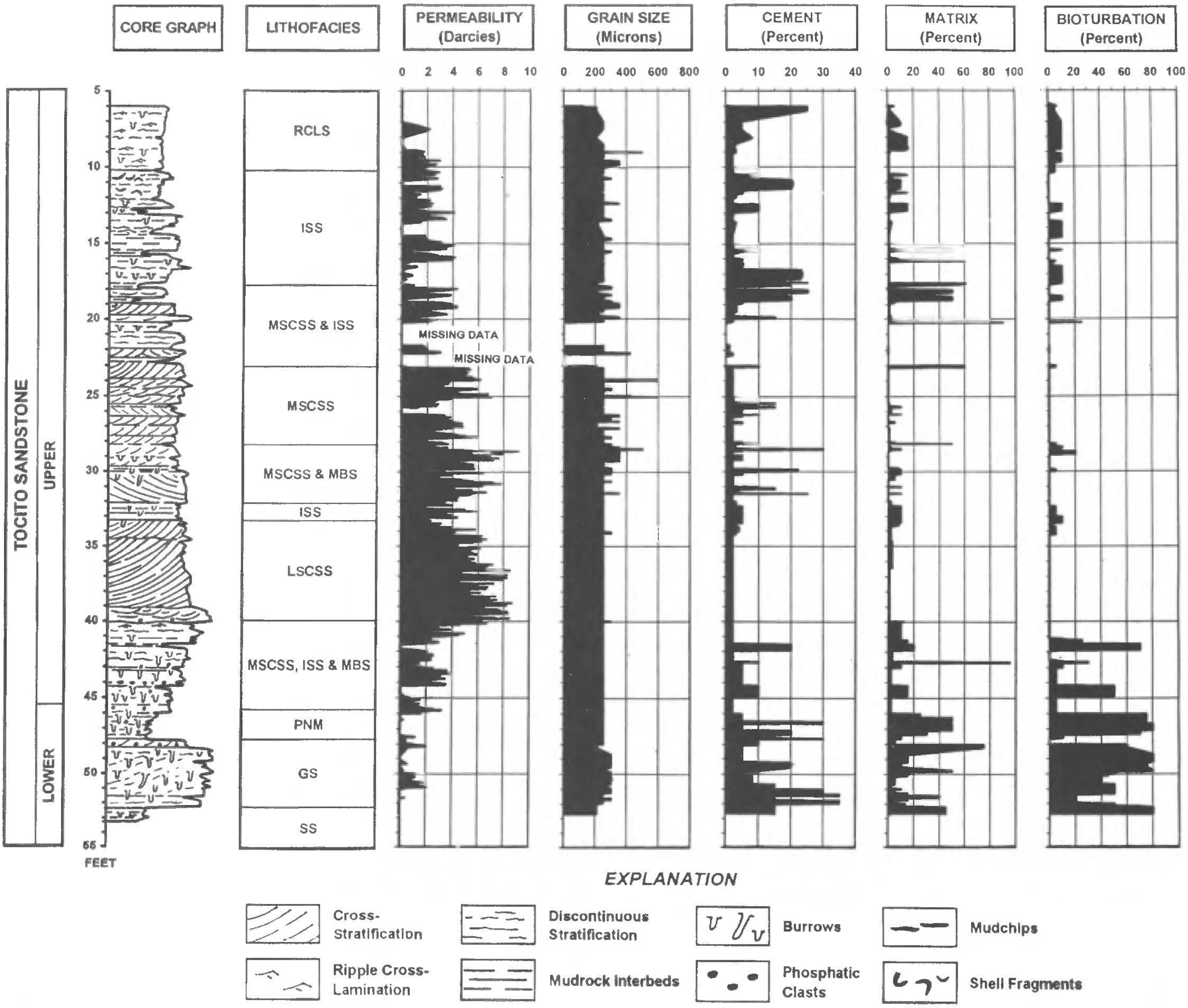

FIGURE 11. Permeability profile for the HOF-2 core at Hogback oil field. Permeability measurements were made with a computer-controlled minipermeameter. Values for grain size, mud and cement content, and degree of bioturbation are visual estimates. Location of core hole is shown on Figure 1.

the sedimentologic characteristics of the F-151 core can be found in Tillman (1985b), Jennette et al. (1991) and Jennette and Jones (1995). Minipermeameter readings with the EPS instrument (N = 51) were taken along the axis of the F-151 core at intervals ranging from 0.1 to 1.0 ft. Permeability values range from 0.001 to 0.275 darcies, with an geometric mean of 0.014 darcies (Table 1). The F-151 permeability profile (Fig. 12) documents the vertical stacking of permeable and non-permeable intervals, similar to what was seen in the shallow core holes (Fig. 11). Overall, the values observed in F-151 are clearly much lower than those from outcrop and shallow core.

RELATIONSHIP OF LITHOFACIES TO PERMEABILITY

Data collected during this study indicate that lithofacies exert a major control over permeability. Comparisons of permeability ranges and median values for various lithofacies in the Tocito are given in Figure 13. The outcrop and shallow-subsurface core data (Fig. 13A) show that the LSCSS and MSCSS lithofacies have superior reservoir characteristics, followed by the ISS, MBS, and RCLS lithofacies. In the deep-subsurface cores (Fig. 13B), the most favorable permeabilities occur in the MSCSS lithofacies, followed by the ISS and MBS lithofacies. The LSCSS and RCLS lithofacies were not evaluated in the deeper cores.

Figure 13 shows that, where comparisons can be made, relative lithofacies rankings for the outcrop and shallow-core data are the same as for the deep subsurface data; however, there is a major difference in the absolute values. Outcrop and shallow-subsurface data for a given lithofacies are two to three orders of magnitude greater than for the same lithofacies in the deep subsurface. Thus, the outcrop observations and statistical characteristics observed at Hogback oil field are portable to the subsurface, although absolute outcrop permeability values are not. Similar conclusions regarding portability between outcrop and subsurface data sets in other depositional systems have been noted by others (e.g., Stalkup and Ebanks, 1986; Goggin et al., 1988a; Chandler et al., 1989; Kittridge et al., 1990; Barton and Tyler, 1991). In the Tocito, the discrepancy between the outcrop and shallow-subsurface values and those from the deep subsurface is due to near-surface physical and chemical weathering, mainly decompaction, micro-fracturing, and dissolution of framework grains and carbonate cement.

SCALES OF RESERVOIR HETEROGENEITY

On a megascopic scale (field-wide scale), the Tocito at Hogback oil field is characterized by interwoven lithofacies with very different permeability structures. Lithofacies of very high permeability (LSCSS and MSCSS) lie

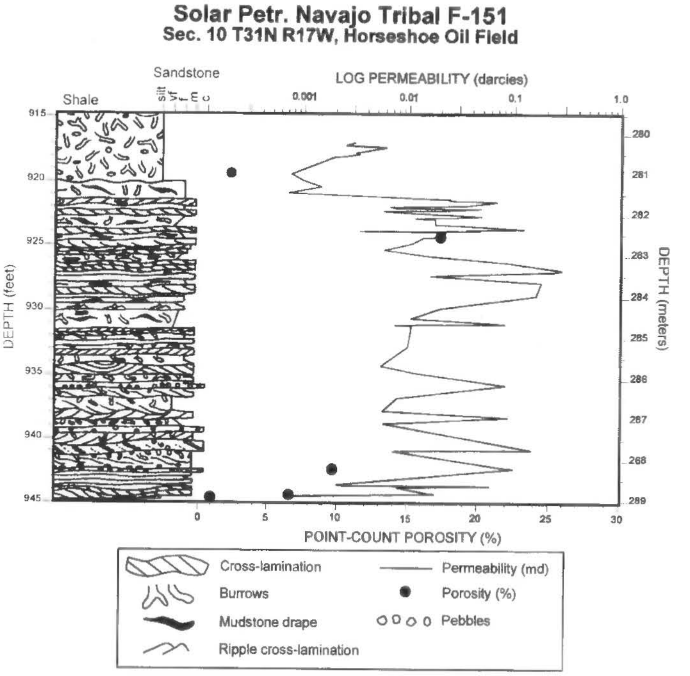

FIGURE 12. Permeability profile for Solar Petroleum Navajo Tribal F-151 from Horseshoe oil field, San Juan Basin (see Fig. 1). Permeability measurements were obtained with the EPS permeameter. Porosity values are based on petrographic observations.

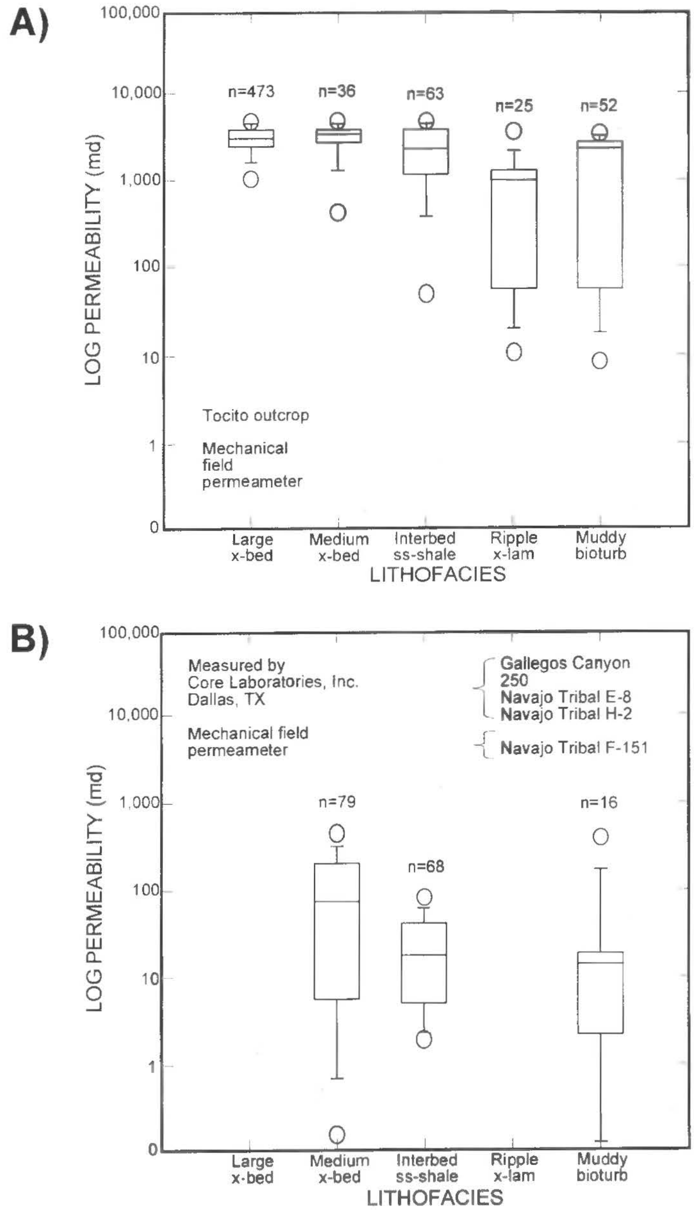

FIGURE 13. Statistical summary (box-and-whisker plots) of permeability values for various Tocito lithofacies in outcrop and the HOF-2 and HOF-3 cores (A), compared to those in deep subsurface cores (B). On the plots, the open circles represent the 5th and 95th percentiles, the small horizontal lines terminating vertical lines represent the 10th and 90 percentiles, and the ends of the large boxes the 25th and 75th percentiles. Horizontal lines in the large boxes represent the 50th percentile values.

among lithofacies with highly variable permeabilities (ISS). At the base of the Tocito is the low-permeability MBS lithofacies and capping the Tocito is the low-permeability RCLS lithofacies. Water injected into a Tocito reservoir would take the path of least resistance, sweeping oil through the cross-bedded sandstone lithofacies and portions of the interbedded lithofacies but bypassing oil retained in the lower permeability lithofacies. Macroscopic scale (well-to-well scale) heterogeneities probably have the most influence on hydrocarbon production in the Tocito Sandstone. Mudstone drapes effectively compartmentalize the main reservoir elements (LSCSS and MSCSS lithofacies). Thus, a well that penetrates and drains three or four stacked sandstone compartments will not drain adjacent compartments. If converted to an injection well, water or steam will not sweep the adjacent compartments. Shale beds within the ISS lithofacies also create compartmentalization at a smaller (mesoscopic) scale. These characteristics suggest that Tocito production would benefit from horizontal drilling.

CONCLUSIONS

Lithofacies are the fundamental control on macroscopic porosity and permeability heterogeneity in the Tocito Sandstone. The MSCSS and LSCSS lithofacies have the highest permeabilities, the ISS lithofacies has intermediate values, and the MBS and RCLS lithofacies have the lowest permeabilities. Mudstone drapes and shale beds have greatly reduced permeabilities and serve to compartmentalize Tocito reservoirs.

Porosity and permeability trends observed in outcrop reflect subsurface conditions. Both the Tocito Sandstone outcrops and the subsurface cores have similar suites of lithofacies, similar hierarchies in relative permeability, and similar permeability trends. Tocito outcrops and shallow subsurface cores have significantly higher porosities and permeabilities than the subsurface Tocito samples, due to decompression during uplift and overburden removal and the additional leaching of framework-grains and calcite cement by meteoric water.

ACKNOWLEDGMENTS

This paper is a brief summary of a Master of Science Thesis prepared by Lambert while at New Mexico Tech. He is indebted to his wife, Cathy, who assisted in the field as well as in the preparation of figures. In addition, he thanks Earl and Donna Lambert and John and Kay Almeida for their emotional and financial support. Additional financial assistance was provided by Mobil Oil, the Society of Economic Paleontologists and Mineralogists/Rocky Mountain Section, the Society of Professional Well Log Analysis Foundation, the Richard Matuzeski Foundation, and Lamb-Fry Oil and Gas in Socorro, NM. Drs. Dave Johnson, Andrew Campbell, John Heller and Neil Whitehead, III, served on the thesis committee along with the two junior authors of this paper, Mozley (thesis committee chair) and Cole.

The Navajo Nation generously provided access to the outcrops and shallow subsurface cores at Hogback oil field. Unocal Corporation provided the EPS and Temco permeameters used in this study. Art Trevena (Unocal), Richard Bottjer (Amoco), Alan Emmendorfer (Giant Exploration and Production) and Steve Semkin (Navajo Community College) helped with various phases of the study. Dr. John Heller provided guidance for use of the computer-controlled minipermeameter at the New Mexico Petroleum Recovery Research Center. Greg Riley and Dag Nummedal provided valuable insight into the lithofacies complexity of the Tocito Sandstone at Hogback oil field. Art Trevena and Martha Cather (PRRC) provided constructive reviews of the manuscript.

REFERENCES

Ali, M., 1993, Small scale heterogeneities in permeability: a correlative study of permeability and corresponding pore morphologies using minipermeameter and petrographic analysis [M. S. thesis]: Socorro, New Mexico Institute of Mining and Technology, 135 p.

Barton, M. D. and Tyler, N., 1991, Quantification of permeability structure in distributary-channel deposits, Ferron Sandstone, Utah; *in* Chidsey, T. C., Jr., ed., Geology of east-central Utah: Utah Geological Association, Publication 19, p. 273–281.

Bottjer, R. J. and Stein, J. A., 1994, Relationship of stratigraphic traps to submarine unconformities: examples from the Tocito Sandstone, San Juan Basin, New Mexico and Colorado; *in* Dolson, J. C., Hendricks, M. L. and Wescott, W. A., eds., Unconformity-related hydrocarbons in sedimentary sequences: Denver, Rocky Mountain Association of Geologists Guidebook, p. 181–208.

Chandler, M. A., Goggin, D. J. and Lake, L. W., 1989, A mechanical field permeameter for making rapid, non-destructive permeability measurements: Journal of Sedimentary Petrology, v. 59, p. 613–635.

Fassett, J. E., Thomaidis, N. D., Matheny, M. L. and Ullrich, R. A., eds., 1987, Oil and Gas Fields of the Four Corners Area, v. 1 and 2: Four Corners Geological Society, 727 p.

Folk, R. L., 1974, Petrology of sedimentary rocks: Austin, Texas, Hemphill, 182 p.

Goggin, D. J., Chandler, M. A., Kocurek, G. and Lake, L. W., 1988a, Patterns of permeability in eolian deposits: Page Sandstone (Jurassic), northeastern Arizona: Society of Petroleum Engineers, Formation Evaluation, p. 297–306.

Goggin, D. J., Thrasher, R. L. and Lake, L. W., 1988b, A theoretical and experimental analysis of minipermeameter response including gas slippage and high velocity flow effects: In Situ, v. 12, no. 1 & 2, p. 79–116.

Heller, J. P., 1992, The PRRC automatic scanning minipermeameter: Socorro, New Mexico Petroleum Recovery Research Center, Paper 92–20.

Jennette, D. C. and Jones, C. R., 1995, Sequence stratigraphy of the Upper Cretaceous Tocito Sandstone: a model for tidally influenced incised valleys, San Juan Basin, New Mexico; *in* Van Wagoner, J. C. and Bertram, G. T., eds., Sequence stratigraphy of foreland basin deposits; outcrop and subsurface examples from the Cretaceous of North America: American Association of Petroleum Geologists, Memoir 64, p. 311–347.

Jennette, D. C., Jones, C. R., van Wagoner, J. C. and Larsen, J. E., 1991, High-resolution sequence stratigraphy of the Upper Cretaceous Tocito Sandstone: the relationship between incised valleys and hydrocarbon accumulation, San Juan Basin, New Mexico; *in* Van Wagoner, J. C., Jones, C. R., Taylor, D. R., Nummedal, D., Jennette, D. C. and Riley, G. W., eds., Sequence stratigraphy applications to shelf sandstone reservoirs; outcrop to subsurface examples: American Association of Petroleum Geologists, Field Conference Guidebook, p.7-24–7-62.

Kittridge, M. G., Lake, L. W., Lucia, F. J. and Fogg, G. E., 1990, Outcrop/subsurface comparisons of heterogeneity in the San Andres Formation: Society of Petroleum Engineers, Formation Evaluation, p. 233–240.

Lambert, M. R., 1993, Controls on porosity and permeability heterogeneity in the Tocito Sandstone (Upper Cretaceous), San Juan Basin, New Mexico [M.S. thesis]: Socorro, New Mexico Institute of Mining and Technology, 265 p.

Lambert, M. R., Mozley, P. S., Cole, R. D. and Riley, G. W., 1995, Facies controlled permeability structure of a highly heterogeneous transgressive-marine complex: Tocito Sandstone, northwest New Mexico; *in* Swift, D. J. P., Snedden, J. W. and Plint, A. G., convenors, Tongues, ridges and wedges; highstand versus lowstand architecture in marine basins: Society of Economic Paleontologists and Mineralogists, Research Conference Program.

Lambert, M. R., Cole, R. D., Mozley, P. S. and Riley, G. W., 1996, Permeability structure of a highly heterogeneous transgressive marine complex: Tocito Sandstone, New Mexico: American Association of Petroleum Geologists, 1996 Annual Convention Official Program, p. A-80.

Molenaar, C. M., 1973, Sedimentary facies and correlation of the Gallup Sandstone and associated formations, northwestern New Mexico; *in* Fassett, J. E., ed., Cretaceous and Tertiary rocks of the Colorado Plateau: Four Corners Geological Society Memoir, p. 85–110.

Molenaar, C. M., 1983a, Major depositional cycles and regional correlations of Upper Cretaceous rocks, southern Colorado Plateau; *in* Reynolds, N. W. and Dolly, E. D., eds., Mesozoic paleogeography of west-central United States: Rocky Mountain Section of Society of Economic Paleontologists and Mineralogists Symposium, no. 2, p. 201–224.

Molenaar, C. M., 1983b, Principal reference section and correlation of Gallup Sandstone, northwestern New Mexico; *in* Contributions to mid-Cretaceous paleontology and stratigraphy of New Mexico, Part II: New Mexico Bureau of Mines and Mineral Resources, Circular 185, p. 29–40.

Molenaar, C. M., Nummedal, D. and Cobban, W. A., 1996, Regional stratigraphic cross sections of the Gallup Sandstone and associated strata around the San Juan Basin, New Mexico, and parts of adjoining Arizona and Colorado: U.S. Geological Survey, Oil and Gas Investigations Chart OC-143.

Nummedal, D. and Molenaar, C. M., 1995, Sequence stratigraphy of ramp-setting strand plain successions: the Gallup Sandstone, New Mexico; *in* Van Wagoner, J. C. and Bertram, G. T., eds., Sequence stratigraphy of foreland basin deposits; outcrop and subsurface examples from the Cretaceous of North America: American Association of Petroleum Geologists, Memoir 64, p. 277–310.

Nummedal, D. and Riley, G. W., 1991, Origin of late Turonian and Coniacian unconformities in the San Juan Basin; *in* Van Wagoner, J. C., Jones, C. R., Taylor, D. R., Nummedal, D., Jennette, D. C. and Riley, G. W., eds., Sequence stratigraphy applications to shelf sandstone reservoirs; outcrop to subsurface examples: American Association of Petroleum Geologists, Field Conference Guidebook, p. 7-63–7-74.

Powers, R. B., 1993, Petroleum exploration plays and resource estimates, 1989, onshore United States; Region 3, Colorado Plateau and Basin and Range: United States Geological Survey, Open-file Report 93-248, 111 p.

Rice, D. D., 1983, Relation of natural gas composition to thermal maturity and source rock type in San Juan Basin, northwestern New Mexico and southwestern Colorado: American Association of Petroleum Geologists Bulletin, v. 67, p. 1199–1218.

Riley, G. W., 1993, Origin of a coarse-grained shallow marine sandstone complex: Coniacian Tocito Sandstone, northwestern New Mexico [Ph.D. dissertation]: Baton Rouge, Louisiana State University, 251 p.

Stalkup, F. I. and Ebanks, W. J., Jr., 1986, Permeability variation in a sandstone barrier island-tidal delta complex, Ferron Sandstone (Lower Cretaceous), central Utah: Society of Petroleum Engineers, Paper 15532, p. 1–8.

Tillman, R. W., 1985a, The Tocito and Gallup Sandstones, New Mexico, a comparison; *in* Tillman, R. W., Swift, D. J. P. and Walker, R. G., eds., Shelf sands and sandstone reservoirs, short course notes 13: Society of Economic Paleontologist and Mineralogists, p. 403–463.

Tillman, R. W., 1985b, Tocito Sandstone core, Horseshoe field, San Juan county, New Mexico; *in* Tillman, R. W., Swift, D. J. P. and Walker, R. G., eds., Shelf sands and sandstone reservoirs, short course notes 13: Society of Economic Paleontologist and Mineralogists, p. 559–576.

Valasek, D., 1995, The Tocito Sandstone in a sequence stratigraphic framework: an example of landward-stepping small-scale genetic sequences; *in* Van Wagoner, J. C. and Bertram, G. T., eds., Sequence stratigraphy of foreland basin deposits; outcrop and subsurface examples from the Cretaceous of North America: American Association of Petroleum Geologists, Memoir 64, p. 349–369.